

Theoretical Studies on the Gas-Phase Alkylation of Delocalized Ambident Anions with Methyl Fluoride

Ikchoon Lee,* Hyung Yeon Park, In-Suk Han, Chang Kon Kim, Chan Kyung Kim, and Bon-Su Lee

Department of Chemistry, Inha University, Incheon 402-751, Korea

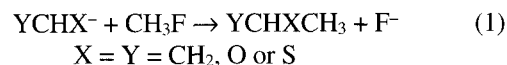
Received November 20, 1998

Gas-phase alkylations of delocalized ambident anions, $Y \cdots CH \cdots X^-$ where $X, Y = CH_2, O, \text{ or } S$, have been investigated theoretically at the MP2/6-31+G*/MP2/6-31+G* and QCISD/6-31+G*/MP2/6-31+G* levels. O- and S-alkylations ($X=O$ and S) are more favored kinetically by $\Delta E^\ddagger = 4.6$ and $9.8 \text{ kcal mol}^{-1}$ than the respective C-alkylations even though they are thermodynamically less favored by 22.4 and $6.0 \text{ kcal mol}^{-1}$ respectively. It was found that the transition structures for the C-alkylations are imbalanced due to the endoergic rehybridization of the carbon center from sp^2 to sp^3 which leads to premature bond contraction of the C-Y bond and delayed bond stretching of the C-X bond. In the O-, or S-alkylation, such endoergic process is not required since the σ -lone pair on O or S is involved in the initial stage of alkylation. The imbalanced TSs for the C-alkylation are accompanied by higher intrinsic barriers and deformation energies.

Introduction

The alkylation of enolate anions in solution is an important class of reaction in organic syntheses.¹ It provides one of the most common ways of forming carbon-carbon bonds (C-alkylation) and also it is used to protect ketones via their vinyl ethers (O-alkylation). Thermodynamically the C-alkylation is expected to be favored since the formation of the C-alkylated product is much more exothermic, by *ca.* $17\text{--}18 (\pm 3) \text{ kcal mol}^{-1}$. For example, thermochemically estimated heats of reactions for the C- and O-alkylations of acetaldehyde enolate anion by methyl fluoride are -12 and $+6 \text{ kcal mol}^{-1}$, respectively,² and those of cyclohexanone enolate anion with methyl bromide are -44 and $-27 (\pm 3) \text{ kcal mol}^{-1}$ respectively.³ These estimates show that the C-alkylation is favored over the O-alkylation by $17\text{--}18 (\pm 3) \text{ kcal mol}^{-1}$ thermodynamically. A similar difference of $\sim 17 \text{ kcal mol}^{-1}$ in the heats of reaction between the gas-phase C- and O-alkylations has also been obtained for the reaction of acetone enolate with trifluoroethyl acetate.⁴ Kinetically, however, O-alkylation has been found to be preferred to C-alkylation in the gas-phase reaction of acetone enolate with methyl chloride and bromide,⁵ and also in the alkylation of cyclohexanone enolate by methyl bromide.³ In contrast, in the gas-phase reaction of acetone enolate anion with trifluoroethyl acetate, only the C-alkylation product was observed,⁴ which was believed to result from the reversible formation of a tetrahedral intermediate; in such case the formation of the thermodynamically preferred C-alkylation product is likely to be favored. On the other hand, O-alkylation is found to dominate in solution unless reactivity of the enolate oxygen is suppressed by coordination of metal cations or protic solvents.⁶ Theoretically, Houk *et al.*, based on the results at the RHF/6-31G*/RHF/3-21G level, predicted O-alkylation rather than C-alkylation for the reaction of acetaldehyde enolate anion with methyl fluoride, even though the latter is favored thermodynamically.² The theoretical as well as

experimental results suggest that the alkylation of enolates proceeds by kinetic control in single-step reactions whereas they are thermodynamically controlled in two-step (or multiple-step) reactions involving a stable intermediate. However, there still remains to be solved the problem of detailed understanding of the causes or reasons for the kinetic control in the enolate alkylation. In view of the importance of alkylation reactions in synthetic chemistry, we attempted to solve the problem by examining the transition structures for the alkylation reactions of delocalized ambident anions with methyl fluoride, eq 1, theoretically at the MP2/6-31+G*/MP2/6-31+G*⁷ and QCISD/6-31+G*/MP2/6-31+G*⁸ levels of theory.



Computational Methods

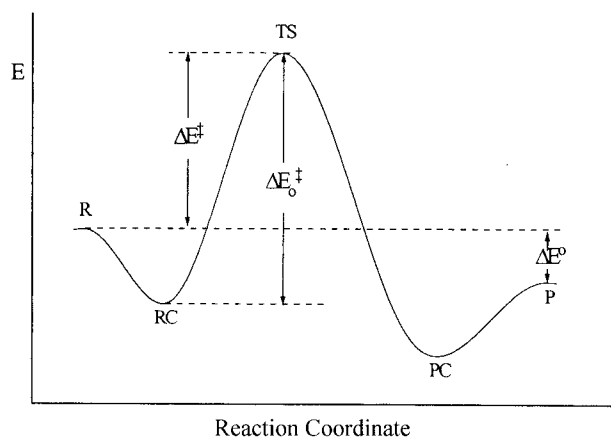
Calculations were carried out with GAUSSIAN-92 and 94 programs.⁹ Since anions are involved, we included a diffuse function and 6-31+G* basis set⁷ was used in all calculations. Geometries were fully optimized. Frequency calculations were performed for all structures, and zero-point vibrational energies (ZPE) and entropies were determined. Electron correlation effects were incorporated at the two levels, MP2 and QCISD.⁸ The latter method was introduced by Pople *et al.*,⁸ by adding quadratic terms in the CISD formalism in order to correct errors arising from size-inconsistent CISD results. We report two types of results: MP2/6-31+G*/MP2/6-31+G* and QCISD/6-31+G*/MP2/6-31+G*.

Free energy (ΔG) and enthalpy changes (ΔH) were determined by eqs 2, where

$$\Delta G = \Delta E + \Delta E(\text{ZPE}) + \Delta H_T + RT - T\Delta S \quad (2a)$$

$$\Delta H = \Delta G + T\Delta S \quad (2b)$$

ΔH_T is the thermal energies involved in the temperature increase from 0 K to 298 K.



Scheme 1

Results and Discussion

Geometries. The gas-phase alkylation reactions of enolate anions with methyl fluoride proceed via a typical S_N2 path-

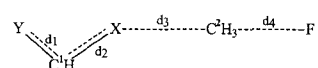
way, and as has been predicted theoretically as well as experimentally a double-well potential energy surface (PES),¹⁰ Scheme 1, was found. The reactant (RC) and product encounter complexes (PC) corresponding to the two wells are ion-dipole types formed by weak electrostatic interactions. Geometries of the reactants and products, RCs and transition structures are summarized in Tables 1~3. Four examples of RCs are shown in Figure 1. We note that the RCs of anions with the same terminal groups *i.e.*, $Y=X$, the structure is not symmetrical with two different distances of d_1 and d_2 between terminal heavy atoms and the methyl carbon, Scheme 2. This is because of two different electrostatic attractions for X_1 (which is eclipsed with H_1) and X_2 (which is staggered with two hydrogens on C_2), Scheme 2; the latter, X_2 , experiences a greater electrostatic attraction by the two hydrogen atoms, H_2 and H_3 , than X_1 which interacts with only one H (H_1). Since the ion-dipole complexes are formed at relatively long distances, the difference in the electrostatic attraction will be small so that the difference in the distance is not large. The distances, d_1 and d_2 , are much

Table 1. Calculated bond lengths (Å) and bond angles (degree) for reactants (CH_3F and anion nucleophiles) and products at the MP2 level

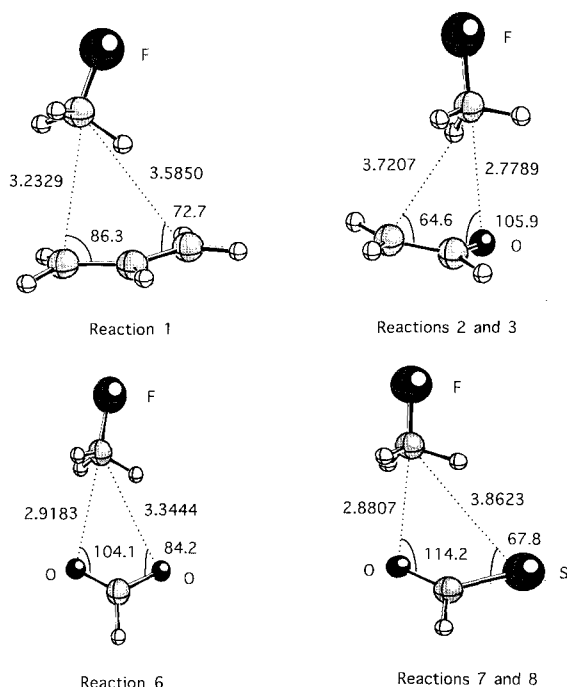
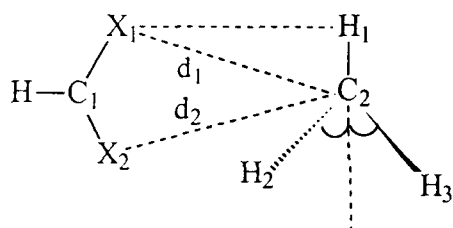
No.	Y	X	R			P				
			d_1	d_2	$\angle YC_1X$	d_1	d_2	d_3	$\angle YC_1X$	$\angle C_1XC_2$
1	CH_2	CH_2	1.3985	1.3985	131.4	1.3426	1.5001	1.5320	124.68	120.0
2	O	CH_2	1.2851	1.3874	129.8	1.2269	1.5110	1.5257	123.74	113.3
3	CH_2	O	1.3874	1.2851	129.8	1.3391	1.3699	1.4302	121.85	114.4
4	S	CH_2	1.7341	1.3634	128.9	1.6231	1.5072	1.5270	125.45	113.2
5	CH_2	S	1.3634	1.7341	128.9	1.3439	1.7594	1.8094	124.32	99.7
6	O	O	1.2681	1.2680	130.2	1.2127	1.3537	1.4431	122.76	115.5
7	S	O	1.7110	1.2538	129.1	1.6177	1.3462	1.4458	123.38	115.6
8	O	S	1.2538	1.7110	129.1	1.2207	1.7629	1.8141	123.72	100.1
9	S	S	1.6822	1.6821	130.2	1.6288	1.7332	1.8138	125.07	100.9
10		$CH_3CH_2^-$		1.5314		1.5269	1.5269			112.3
11		CH_3O^-		1.3610		1.4202	1.4202			111.4
12		CH_3S^-		1.8336		1.8064	1.8064			98.4

Table 2. Calculated bond lengths (Å) and bond angles (degree) of reactant complexes (RCs) at the MP2 level

No.	Y	X	d_1	d_2	d_3	d_4	$\angle YC_1X$	$\angle C_1XC_2$	$\angle XC_2F$
			d_1	d_2	d_3	d_4	$\angle YC_1X$	$\angle C_1XC_2$	$\angle XC_2F$
1	CH_2	CH_2	1.3971	1.4002	3.2329	1.4385	130.8	86.3	164.9
2	O	CH_2	1.2889	1.3849	3.7211	1.4424	129.0	64.6	137.7
3	CH_2	O	1.3849	1.2889	2.7777	1.4424	129.0	105.9	177.4
4	S	CH_2	1.7337	1.3640	3.7377	1.4361	128.7	76.2	171.5
5	CH_2	S	1.3640	1.7337	3.3986	1.4361	128.7	84.3	171.7
6	O	O	1.2682	1.2699	2.9183	1.4420	129.4	104.1	177.7
7	S	O	1.7076	1.2569	2.8807	1.4361	128.6	114.2	175.3
8	O	S	1.2569	1.7076	3.8623	1.4361	128.6	67.8	139.4
9	S	S	1.6814	1.6836	3.4536	1.4316	130.1	90.3	175.2
10		$CH_3CH_2^-$		1.5320	3.1936	1.4525		85.6	166.4
11		CH_3O^-		1.3658	2.6922	1.4487		114.4	179.7
12		CH_3S^-		1.8310	3.3383	1.4392		85.6	169.6

Table 3. Calculated bond lengths (Å) and bond angles (degree) of transition structures at the MP2 level


No.	Y	X	d_1	d_2	d_3	d_4	$\angle YC^1X$	$\angle C^1XC^2$	$\angle XC^2F$
1	CH ₂	CH ₂	1.3749	1.4253	2.2331	1.7346	128.6	103.2	176.8
2	O	CH ₂	1.2623	1.4139	2.1468	1.8210	127.7	101.4	176.3
3	CH ₂	O	1.3643	1.3141	1.8633	1.8559	127.3	112.7	178.7
4	S	CH ₂	1.6747	1.4029	2.0372	1.8926	127.5	102.9	175.2
5	CH ₂	S	1.3549	1.7388	2.2905	1.8898	128.2	96.2	179.3
6	O	O	1.2440	1.2977	1.8206	1.9180	127.1	117.9	178.3
7	S	O	1.6620	1.2882	1.7717	1.9643	126.6	117.1	178.9
8	O	S	1.2407	1.7264	2.2333	1.9605	128.4	102.1	177.2
9	S	S	1.6569	1.7001	2.2126	1.9520	130.0	105.7	175.6
10		CH ₃ CH ₂ ⁻		1.5249	2.4727	1.6302		98.5	174.6
11		CH ₃ O ⁻		1.3791	1.9835	1.7357		107.6	178.8
12		CH ₃ S ⁻		1.8179	2.3496	1.8411		92.8	178.2

**Figure 1.** Optimized Structures of the Reactant Complexes at the MP2 level.**Scheme 2**

large for X=S than for X=O since the former being a second-row element has a relatively large covalent radius. In contrast, for X=CH₂ steric repulsions between hydrogens on X and on the substrate (CH₃) are expected, which may be one of the factors for longer distances (d_1 and d_2) for X=CH₂ than X=O in addition to a much stronger interactions

Table 4. Proton affinities (PA) and methyl cation affinities (MCA) at the MP2 level (kcal mol⁻¹)

No.	Y	X	PA	MCA
1	CH ₂	CH ₂	-398.7	-299.4
2	O	CH ₂	-372.3	-271.5
3	CH ₂	O	-356.6	-247.8
4	S	CH ₂	-352.9	-252.1
5	CH ₂	S	-344.3	-245.7
6	O	O	-342.2	-229.3
7	S	O	-330.1	-218.7
8	O	S	-331.9	-232.5
9	S	S	-326.3	-227.8
10		CH ₃ CH ₂ ⁻	-429.6	-330.2
11		CH ₃ O ⁻	-384.4 (-379) ^a	-278.8
12		CH ₃ S ⁻	-358.1 (-359)	-260.7

^aExperimental values, Ref. 7, p 314.

expected between O and CH₃ due to a stronger electronegativity of O. The structures of PCs are of little interest and importance. The transition structures will be discussed later on separately.

Proton Affinities (PA) and Methyl Cation Affinities (MCA). For each reaction center, X and Y, on the ambident anions, proton affinities (PA), eq 3, and methyl cation affinities (MCA), eq 4, are determined as listed in Table 4.

$$PA = E(XCHYH \text{ or } YCHXH) - \{E(YCHX^-) + E(H^+)\} \quad (3)$$

$$MCA = E(XCHYCH_3 \text{ or } YCHXCH_3) - \{E(YCHX^-) + E(CH_3^+)\} \quad (4)$$

These two quantities represent a measure of nucleophilicity of each reaction center of the anion nucleophiles.^{10a,c} The PAs and MCAs of localized anion nucleophiles are considerably greater than those of the corresponding delocalized anion centers. The PAs and MCAs decrease in the order X = CH₂ > O > S under the same structural changes, e.g., CH₂CHCH₂⁻ > CH₂CHO⁻ > CH₂CHS⁻, etc.

Energetics. The energies and energy differences relative to the reactant complex (RC) and

$$\text{Central barrier, } \Delta E_c^\ddagger = E^\ddagger - E_{RC} \quad (5a)$$

Table 5. Calculated activation, complexation and reaction energies for the S_N2 reactions in kcal mol⁻¹

No.	Y	X	E_R^a	RC			ΔE^\ddagger_c	TS			PS			P		
				ΔE_{RC}^b	-	ΔG_{RC}		ΔE^\ddagger_b	$-T\Delta S^\ddagger$	ΔG^\ddagger	ΔE_{PC}	$T\Delta S_{PC}$	ΔG_{PC}	ΔE^O	$-T\Delta S^O$	ΔG^O
1	CH ₂	RHF	-255.46943	-6.9	6.9	1.3	24.2	17.3	10.0	28.0	-10.8	7.6	-2.4	-37.4	2.2	-32.1
		RMP2	-256.18102	-9.2	9.4	1.8	12.4	3.2	11.6	15.7	-12.6	7.7	-4.0	-45.9	3.6	-39.0
		QCISC	-256.23067	-8.6		2.4	14.0	5.4		17.8	-14.2		-4.5	-44.1		-37.1
2	O	RHF	-291.35588	-9.0	4.7	-3.0	33.6	24.7	9.8	34.7	-19.3	6.6	-10.8	-11.0	2.6	-7.5
		RMP2	-292.11824	-10.8	7.7	-1.7	21.7	11.0	10.2	21.7	-20.1	6.8	-11.6	-18.1	2.7	-14.1
		QCISC	-292.15602	-10.6		-1.5	24.1	13.5		24.2	-20.3		-12.0	-17.4		-13.4
3	CH ₂	RHF	-291.35588	-9.0	4.7	-3.0	29.0	20.1	9.2	30.0	-18.5	5.2	-11.7	11.7	2.6	-15.6
		RMP2	-292.11824	-10.8	7.7	-1.7	19.0	8.2	9.3	18.1	-19.9	6.9	-11.4	5.6	2.7	9.4
		QCISC	-292.15602	-10.6		-1.5	19.5	8.9		18.8	-19.7		-10.9	5.0		8.8
4	S	RHF	-614.03454	-6.7	5.7	0.2	46.6	39.9	10.1	49.7	-22.7	6.8	-14.1	18.5	2.7	21.2
		RMP2	-614.72796	-9.1	7.4	-0.5	29.5	20.4	10.3	30.8	-22.0	6.9	-13.4	1.4	2.8	4.6
		QCISC	-614.77879	-8.6		0.0	33.1	24.5		34.9	-22.3		-13.7	3.4		6.7
5	CH ₂	RHF	-614.03454	-6.3	5.8	0.7	34.7	28.4	8.6	36.8	-19.2	7.1	-10.5	22.5	2.2	24.2
		RMP2	-614.72796	-9.1	7.4	-0.5	22.2	13.1	9.1	21.9	-21.9	7.4	-12.9	7.7	2.2	9.5
		QCISC	-614.77879	-8.6		0.0	23.4	14.7		23.5	-21.3		-13.9	9.4		11.2
6	O	RHF	-227.53397	-9.2	6.5	-1.4	34.7	25.5	9.0	34.9	-26.8	8.5	-17.0	29.8	1.2	32.2
		RMP2	-228.03716	-10.8	6.8	-2.8	25.6	14.8	8.9	24.2	-28.2	9.1	-18.0	24.1	0.7	25.9
		QCISC	-228.04299	-10.8		-2.8	26.5	15.7		25.0	-28.4		-18.2	24.5		26.3
7	S	RHF	-550.18661	-7.4	6.0	-0.2	42.3	34.9	9.5	44.6	-30.1	8.6	-20.2	48.7	1.4	50.9
		RMP2	-550.62398	-9.5	6.9	-1.4	30.0	20.6	8.3	29.0	-28.9	8.7	-19.0	34.8	1.2	36.7
		QCISC	-550.64217	-9.3		-1.2	31.2	22.0		30.5	-29.4		-19.5	36.2		38.1
8	O	RHF	-550.18661	-7.5	5.9	-0.4	40.4	32.9	8.0	40.5	-27.8	8.5	-18.1	35.4	1.1	36.2
		RMP2	-550.62398	-9.5	6.9	-1.4	27.9	18.4	9.3	27.3	-29.2	9.2	-19.0	20.9	0.6	21.3
		QCISC	-550.64217	-9.3		-1.2	29.2	20.0		28.9	-28.7		-18.5	22.5		22.8
9	S	RHF	-872.83244	-6.3	5.3	0.1	44.2	37.9	9.4	46.8	-29.4	8.6	-19.7	43.3	1.4	44.2
		RMP2	-873.21094	-8.5	7.1	-0.2	29.8	21.3	9.1	29.8	-30.1	8.9	-19.4	25.6	1.0	26.1
		QCISC	-873.23997	-8.1		0.3	31.4	23.3		31.9	-19.7		-19.5	27.9		28.4
10	CH ₂	RHF	-217.58888	-8.0	5.0	-1.9	12.7	4.7	10.6	15.0	-6.7	6.8	0.9	-67.7	2.7	-61.8
		RMP2	-218.18255	-9.6	6.7	-2.0	3.2	-6.4	8.7	2.0	-9.0	7.1	-1.0	-76.7	2.7	-70.9
		QCISC	-218.22800	-9.5		-1.9	2.6	-5.3		3.2	-8.9		-0.7	-74.2		-68.4
11	O	RHF	-253.47448	-11.5	7.2	-4.3	18.6	7.1	8.8	16.9	-10.7	6.9	-2.8	-20.5	1.5	-16.2
		RMP2	-254.12020	-13.1	6.1	-5.8	8.3	-4.8	9.1	5.1	-13.1	7.2	-4.9	-25.4	1.5	-21.3
		QCISC	-254.15546	-13.2		-5.9	9.3	-3.8		6.1	-13.1		-4.7	24.6		-20.5
12	S	RHF	-576.18305	-7.1	7.0	-0.1	30.5	23.4	8.2	31.2	-14.4	7.4	-5.9	-10.0	1.2	11.2
		RMP2	-576.75370	-9.2	5.5	-2.6	16.4	7.2	8.3	15.2	-16.9	7.7	-8.1	-7.3	1.1	-6.0
		QCISC	-576.80118	-9.0		-2.3	18.0	9.0		17.1	-16.5		-7.9	-4.5		-3.2

^aReactant energy in hartree. ^bCorrected for zero point energies (ZPE).

$$\text{Activation energy, } \Delta E^\ddagger = E^\ddagger - E_R \quad (5b)$$

$$\text{Reaction energy, } \Delta E^o = E_P - E_R \quad (5c)$$

separated reactants R, eqs 5, are summarized in Table 5. For comparison with experimental results, enthalpy changes, ΔH (eq (2b)), and Gibbs free energy changes, ΔG^\ddagger and ΔG^o (eq (2a)) are determined. We point out that the MO theoretical transition structures and the TS structures are not necessarily the same.¹²

Reference to Table 5 reveals that the heats of reactions, ΔH^o , for reactions 2 (OCHCH₂⁻ + MeF) and 3 (CH₂CHO⁻ + MeF) are -16.8 and +6.7 kcal mol⁻¹ by MP2 and -16.1 and +6.1 kcal mol⁻¹ by QCISC, which compare well with the estimated values based on the experimental data, -12 and +6

kcal mol⁻¹ considering the 1~5 kcal mol⁻¹ errors in the estimates. The QCISC values are in better agreement, albeit the improvement is marginal. Our results are much better than those predicted based on the lower level computational results: the two values are +33.9 and +47.9 kcal mol⁻¹ at the RHF/3-21G//RHF/3-21G level and +9.5 and +32.7 kcal mol⁻¹ at the RHF/6-31G**//RHF/3-21G level.² These lower level results predicted even incorrect signs for the ΔH^o values of reaction 2. Interestingly, the gas-phase reactions of cyclohexanone enolate with CH₃Br³ and acetone enolate with CH₃COCH₂CF₃⁴ both predicted *ca.* 17±3 kcal mol⁻¹ difference in ΔH^o between the C- and O-alkylation with a greater exothermicity for the C-alkylation. Our QCISC result of ~22 kcal mol⁻¹ for the reactions of acetaldehyde enolate

anion with CH_3F is thus in good agreement.

Examination of Table 5 shows that both the activation (ΔE^\ddagger and ΔG^\ddagger) and reaction energies (ΔE° and ΔG°) increase in the order $\text{CH}_3\text{CH}_2^- < \text{CH}_3\text{O}^- < \text{CH}_3\text{S}^-$ for the localized anion nucleophiles, reactions 10~12. Thus the greater the thermodynamic driving force ($\delta\Delta E^\circ < 0$), the greater is the reactivity ($\delta\Delta E^\ddagger < 0$), indicating that the rates of alkylation are thermodynamically controlled. In contrast, however the alkylations of delocalized ambident anions OCHCH_2^- and SCHCH_2^- with CH_3F are predicted to proceed by the O- or S-alkylations (reactions 3 and 5) with lower activation barriers than the corresponding C-alkylations (reactions 2 and 4) even though the C-alkylations are thermodynamically favored with greater thermodynamic driving force. This means that the alkylation rates of delocalized anions OCHCH_2^- and SCHCH_2^- with CH_3F are kinetically controlled, which is in contrast to the thermodynamically controlled alkylations of the localized anions, reactions 10~12. Since the alkylations of delocalized anions OCHCH_2^- and SCHCH_2^- are kinetically controlled, there is no proportionality between the activation barrier, ΔE^\ddagger , and the exothermicity of reaction, ΔE° , as required for the reactions with the same reaction center, X, by the Leffler-Hammond rate-equilibrium relation or Bell-Evans-Polanyi (BEP) principle,¹⁴ eq 6. According to the Marcus equation,^{10,11,15} eq (7), the activation barrier ΔE^\ddagger is determined by the intrinsic (or kinetic) barrier, ΔE_o^\ddagger , and

$$\delta\Delta E^\ddagger = \alpha\delta\Delta E^\circ \quad (6)$$

$$\Delta E^\ddagger = \Delta E_o^\ddagger + \frac{1}{2}\Delta E^\circ + \frac{(\Delta E^\circ)^2}{16\Delta E_o^\ddagger} \quad (7)$$

thermodynamic driving force (ΔE°). The alkylations of delocalized anions OCHCH_2^- and SCHCH_2^- are therefore controlled by the intrinsic barriers, ΔE_o^\ddagger , rather than by ΔE° . On the other hand, the relative reactivities depending on the heavy atoms are invariably in the order $\text{S} < \text{O} < \text{CH}_2$ under the same condition; for example, keeping the Y group to CH_2 , ΔE^\ddagger decreases in the order $\text{X} = \text{S}(14.7) > \text{O}(8.9) > \text{CH}_2(5.4 \text{ kcal mol}^{-1})$ and similarly keeping the X to O, ΔE^\ddagger decreases in the same order $\text{Y} = \text{S}(22.0) > \text{O}(15.7) > \text{CH}_2(8.9 \text{ kcal mol}^{-1})$. This reactivity order is the same as that found for the localized anions (reactions 10~12) and seems to reflect the increasing order of thermodynamic driving force ($\delta\Delta E^\circ < 0$).

Transition Structures. It is commonly accepted that the slopes of the plots of ΔE^\ddagger vs PA, eq 8, and of ΔE^\ddagger vs MCA, eq 9, provide a measure of the degree of progress of reaction,^{10,13b,16} which is the degree of bond making between the reaction center X and methyl carbon of MeF in the alkylation reactions or in $\text{S}_\text{N}2$ reactions. Another such measure is

$$\delta\Delta E^\ddagger = \beta \cdot \alpha \text{ PA} \quad (8)$$

$$\delta\Delta E^\ddagger = \beta' \cdot \delta\text{MCA} \quad (9)$$

of course the α in eq 6. The slopes, α , β and β' , are collected in Table 6. Based on the averages of these three parameters, the C-, O- and S-alkylations are predicted to be progressed ca. 34, 44, 45% respectively in the transition structures. The O- and S-alkylations are progressed to nearly the same

Table 6. The Values of α , β and β'

Reactions	α	β	β'	average	For reaction centers, X=
1, 2, 4, 10	0.369	0.335	0.328	0.344	CH_2
3, 6, 7, 11	0.423	0.480	0.425	0.443	O
5, 8, 9, 12	0.466	0.448	0.428	0.447	S

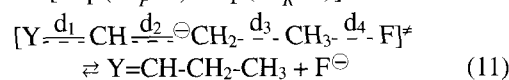
Table 7. Percentage changes of bond orders, $\% \Delta n^\ddagger$

No.	Y	X	d_1	d_2	d_3	d_4
1	CH_2	CH_2	40.6 (42.9) ^a	29.0 (25.7) ^a	31.1 (34.4) ^b	42.1
2	O	CH_2	37.4 (39.7)	25.4 (21.8)	35.5 (34.4)	49.8
3	CH_2	O	45.9 (47.9)	37.3 (34.1)	48.6 (44.3)	52.7
4	S	CH_2	48.5 (53.2)	32.7 (27.8)	42.7 (34.4)	55.5
5	CH_2	S	41.3 (42.1)	20.7 (20.0)	44.8 (44.7)	55.3
6	O	O	41.4 (43.6)	38.2 (34.9)	53.3 (44.3)	57.3
7	S	O	48.8 (52.7)	40.6 (37.0)	58.1 (44.3)	60.5
8	O	S	38.1 (39.4)	30.7 (28.9)	49.7 (44.7)	60.3
9	S	S	45.0 (47.2)	37.3 (35.3)	51.4 (44.7)	59.7
10		CH_3CH_2^-		150.5 (150.0)	20.7 (34.4)	31.0
11		CH_3O^-		32.6 (30.5)	39.1 (44.3)	42.2
12		CH_3S^-		48.8 (50.0)	40.4 (44.7)	51.5

^a $\% \Delta d^\ddagger = (\Delta d^\ddagger / \Delta d^\circ) \times 100$ where $\Delta d^\ddagger = d^\circ - d_R$ and $\Delta d^\circ = d_P - d_R$. ^bThe values in parentheses are the averages of percentage bond length change in the TS taken from Table 6.

degree, in contrast to a significantly lesser (ca. 10% less) degree of bond making in the C-alkylation. Percentage bond length changes in the transition structures can be estimated by using bond lengths, $\% \Delta d^\ddagger = (\Delta d^\ddagger / \Delta d^\circ) \times 100$, and bond orders $\% \Delta n^\ddagger$, eq 10,¹⁷ where d^\ddagger , d_P and d_R represent bond length in the transition structure (\ddagger), product (P) and reactant (R), respectively, and $\Delta d^\ddagger = d^\ddagger - d_R$ and $\Delta d^\circ = d_P - d_R$. The parameter a can be either 0.3 for normal bonds or 0.6 for partial bonds.¹⁷ The results of percentage bond length changes in the transition structures, $\% \Delta d^\ddagger$ and $\% \Delta n^\ddagger$, are summarized in Table 7. Examination of Table 7 reveals that in the transition structure of C-alkylation contraction of d_1 is more advanced whereas stretching of d_2 lags behind the progress of reaction represented by the degree of bond formation d_3 between X and methyl carbon, eq 11. This type of

$$\% \Delta n^\ddagger = \frac{[\exp(-d^\ddagger/a) - \exp(-d_R/a)]}{[\exp(-d_P/a) - \exp(-d_R/a)]} \times 100 \quad (10)$$



imbalanced transition structure is a manifestation of the principle of nonperfect synchronization (PNS)¹⁸ and leads to an increase in the intrinsic barrier, ΔE_o^\ddagger . According to the PNS, a product stabilizing factor, such as resonance or solvation etc., that develops late along the reaction coordinate, or a reactant stabilizing factor that is lost early always lowers the intrinsic rate of reaction, k_o , or alternatively elevates the intrinsic barrier, ΔE_o^\ddagger .¹⁸ A typical system where there is a lack of synchronization is the deprotonation of carbon acids activated by π -acceptors, CH_3CHO or CH_3NO_2 , where charge transfer into the π -acceptor lags behind the proton

transfer. A consequence of the lag in charge delocalization is that there is little development of resonance stabilization in the TS, which is the major reason why reactions that lead to resonance-stabilized products have high intrinsic barriers. The forward reaction of eq 11, *i.e.*, C-alkylation of a delocalized enolate anion, corresponds to a reverse process of the deprotonation of a carbon acid, where resonance develops prematurely in advance, or early, along the reaction coordinate than the progress of reaction which is the degree of protonation or the degree of bond formation in the C-alkylation. We note that in the C-alkylation contraction of d_1 or double bond formation is ahead of bond making process of d_3 , $\% \Delta d_1^\ddagger > \% \Delta d_3^\ddagger$. This imbalance should be the cause of an increase in the intrinsic barrier, ΔE_o^\ddagger , for the C-alkylation leading to slower rates than O-alkylation or S-alkylation for which no such TS imbalances are found. For example, in the C-alkylation (reaction 2) d_1 has changed 37% in contrast to 35% progress in the bond making of d_3 , whereas in the O-alkylation (reaction 3) d_1 has changed 46% but d_3 has changed 49%. Similarly in the C-alkylation (reaction 4) d_1 has progressed to 49% in contrast to the 43% bond making, whereas in the S-alkylation (reaction 5) it is 41% (d_1) vs 45% (d_3). This is reasonable since in the C-alkylation bond contraction of d_1 involves a change of a single \rightarrow double bond which is exothermic so that proceeds ahead of bond making, whereas stretching of d_2 involves rehybridization of carbon center ($X=CH_2$) from sp^2 to sp^3 which is an endothermic process²⁰ so that lags behind the bond making. In the O-alkylation, however, progress of bond contraction of d_1 (46%) and bond stretching of d_2 (37%) are less than the bond making (49%). However, in the bond stretching no rehybridization is required since the reaction center is an oxygen atom which utilizes a σ lone-pair in the initial stage of bond making. Thus there is no TS imbalance ($\% \Delta d_1^\ddagger > \% \Delta d_3^\ddagger$) and there is no incipient energy costing rehybridization. Situation is similar with the C-alkylation (reaction 4) *versus* S-alkylation (reaction 5); in the former the TS becomes imbalanced and there is no incipient endoergic rehybridization in the latter.

It is therefore clear that the preference of O-alkylation (or S-alkylation) to the C-alkylation is due to the imbalanced TS in the latter in which there occurs an intrinsic-barrier elevation incurred by the imbalanced TS and the endoergic rehybridization of reaction center carbon of the delocalized anion, in contrast to no such effects in the former, O- or S-alkylation.

A greater intrinsic barrier, ΔE_o^\ddagger , for the C-alkylation can be shown directly by estimating the ΔE_o^\ddagger values for the two delocalized ambident anion centers using the well established relation, eq 12,¹¹ where $\Delta E_o^\ddagger(X, Y)$ is the intrinsic barrier for the non-identity reactions, eq 13, and $\Delta E_o^\ddagger(X, X)$

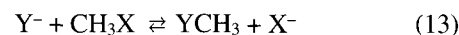
$$\Delta E_o^\ddagger(X, Y) = \frac{1}{2} (\Delta E_o^\ddagger(X, X) + \Delta E_o^\ddagger(Y, Y)) \quad (12)$$

and $\Delta E_o^\ddagger(Y, Y)$ are the intrinsic barriers (in the thermoneutral, identity reactions).¹¹ Using the $\Delta E_o^\ddagger(F, F)$ value of 12.6 kcal mol⁻¹,¹⁹ which was determined at a theoretical level

Table 8. Calculated (eq 12) intrinsic barriers of delocalized anions in the methyl transfer reactions (based on $\Delta E_o^\ddagger(F, F)=12.6$ kcal mol⁻¹)

	ΔE_o^\ddagger (kcal mol ⁻¹)	DE (kcal mol ⁻¹) ^d
F ⁻	12.6 ^a (26.2 ^b , 11.7 ^c)	-
CH ₃ O ⁻	6.0 (26.2 ^b)	-
CH ₃ S ⁻	23.4 (24.2 ^b)	-
CH ₂ CHCH ₂ ⁻	15.4	1.5
OCHCH ₂ ⁻	35.6	2.0
CH ₂ CHO ⁻	26.4	0.9
SCHCH ₂ ⁻	53.6	4.5
CH ₂ CHS ⁻	34.8	0.1
OCHO ⁻	40.4	-
SCHO ⁻	49.8	-
OCHS ⁻	45.8	-
SCHS ⁻	50.2	-

^aAt the MP2/6-31++G**//RHF/6-31++G** level.¹⁹ ^bGas-phase experimental value.¹⁰ ^cAt the RHF/4-31G level.^{11a} ^dDeformation energy = (Energy of the anion nucleophile at the transition-structure geometry) - (Energy of the anion nucleophile reactant) at the MP2 level.



similar to that was used in the present work (MP2/6-31++G**//RHF/6-31++G**), and $\Delta E_c^\ddagger \approx \Delta E_o^\ddagger(X, Y)$ the $\Delta E_o^\ddagger(Y, Y)$ values are estimated using eq 12 as shown in Table 8. We note in the Table that the C-alkylation is expected to lead to a higher intrinsic barrier than the O- or S-alkylation; the ΔE_o^\ddagger values for the C-alkylation, OCHCH₂⁻, and O-alkylation, CH₂CHO⁻, are 35.6 and 26.4 kcal mol⁻¹, the intrinsic barrier to the C-alkylation is higher by *ca.* 10 kcal mol⁻¹. A similar comparison shows that the C-alkylation has a higher intrinsic barrier by *ca.* 20 kcal mol⁻¹ than the S-alkylation.

In the gas-phase identity reactions of $X^- + CH_3X$ with $X=CH_3COCH_2$ the intrinsic barriers, ΔE_o^\ddagger , were ~ 29 and 15 kcal mol⁻¹ for the C- and O-alkylations,^{10,22} respectively, with $\delta \Delta E_o^\ddagger \approx 14$ kcal mol⁻¹. Our estimate of the intrinsic barrier difference $\delta \Delta E_o^\ddagger \approx 10$ kcal mol⁻¹ therefore, seems to be reasonable, albeit in our reaction system $X=HCOCH_2$.

The deformation energies (DE) representing the endoergic rehybridization show that the C-alkylations have invariably higher deformation energies than the corresponding O- or S-alkylation. There is a parallel change in ΔE_o^\ddagger and DE.

We have shown the transition structures for the reactions 1~5 in Figure 2. There is an apparent pyramidalization of the reaction center carbon in the C-alkylation corresponding to the endoergic rehybridization of $sp^2 \rightarrow sp^3$, which is absent in the O- or S-alkylation. In the C-alkylation the two molecular planes, π -orbital plane of the delocalized anions and methyl plane, are approximately parallel indicating a π -attack, whereas in the O- or S-alkylation the molecular plane of the delocalized anion approaches CH₃ plane bisecting an HCH angle in a σ -approach where one of the two σ -lone pairs approach methyl carbon in the transition structure. Thus there is no need for an incipient endoergic rehybridiza-

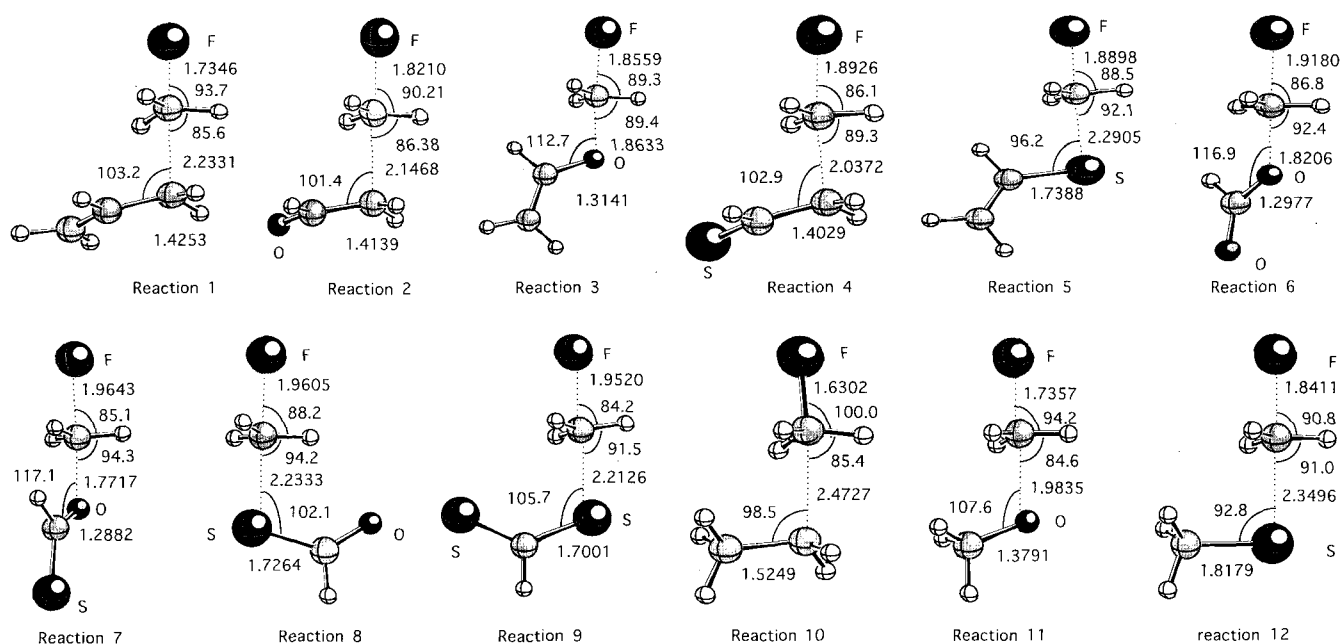


Figure 2. Optimized Transition Structures at the MP2 level.

tion of $sp^2 \rightarrow sp^3$ at the reaction center of the delocalized anion.

We conclude that the activation barrier, ΔE^\ddagger , for the C-alkylation is higher than that for the O- or S-alkylation mainly due to the elevated intrinsic barrier, ΔE_o^\ddagger , which is incurred by the imbalanced TS of the more advanced charge transfer to effect early bond contraction by an exoergic process of $sp^3 \rightarrow sp^2$ and of the lag in bond stretching by the endoergic $sp^2 \rightarrow sp^3$ rehybridization of the reaction center carbon atom which leads to the lag in bond stretching.

Acknowledgment. We thank Inha University and MOST-FOTD project for support of this work. We also thank the SERI for computing facility of CRAY T3E supercomputer.

References

- (a) March, J. *Advanced Organic Chemistry*, 2nd ed.; McGraw-Hill: New York: 1977; p 336 and 418. (b) House, H. O. *Modern Synthetic Reactions*, 2nd ed.; Benjamin, W. A., Ed.; Menlo Park, CA, 1972; p 492. (c) Gompper, R.; Wagner, H.-U. *Angew. Chem. Int. Ed. Engl.* **1976**, *15*, 321.
- Houk, K. N.; Paddon-Row, M. N. *J. Am. Chem. Soc.* **1986**, *108*, 2659.
- Jones, M. E.; Kass, S. R.; Filley, J.; Barkley, R. M.; Ellison, G. B. *J. Am. Chem. Soc.* **1985**, *107*, 109.
- Bartmess, J. E.; Hays, R. L.; Caldwell, G. *J. Am. Chem. Soc.* **1981**, *103*, 1338.
- Bohme, D. K.; Raksit, A. B. *J. Chem. Soc.* **1980**, *106*, 5993.
- (a) Jackman, L. M.; Lange, B. C. *J. Am. Chem. Soc.* **1981**, *103*, 4494. (b) Jackman, L. M.; Dunne, T. J. *J. Am. Chem. Soc.* **1985**, *107*, 2805. (c) Klopman, G. In *Chemical Reactivity and Reaction Paths*; Klopman, G., Ed.; Wiley-Interscience: New York, 1974; p 77.
- Hehre, W. J.; Radom, L.; Schleyer, P. v. R.; Pople, J. A. *Ab Initio Molecular Orbital Theory*; Wiley: New York, 1986, Chapter 4.
- Pople, J. A.; Head-Gordon, M.; Raghavachari, K. *J. Chem. Phys.* **1987**, *87*, 5968.
- (a) Frisch, M. J.; Trucks, G. W.; Head-Gordon, M.; Gill, P. M. W.; Wong, M. W.; Foresman, J. B.; Johnson, B. G.; Schlegel, H. B.; Robb, M. A.; Replogle, E. S.; Gomperts, R.; Andres, J. L.; Raghavachari, K.; Binkley, J. S.; Gonzalez, C.; Martin, R. L.; Fox, D. J.; Defress, D. J.; Baker, J.; Stewart, J. J. P.; Pople, J. A. Gaussian 92, Revision A; Gaussian Inc.: Pittsburgh, PA, 1992. (b) Frisch, M. J.; Trucks, G. W.; Schlegel, H. B.; Gill, P. M. W.; Johnson, B. G.; Robb, M. A.; Chessemann, J. R.; Keith, T. A.; Petersson, G. A.; Montgomery, J. A.; Raghavachari, K.; Al-Laham, M. A.; Zakrzewski, V. G.; Ortiz, J. V.; Foresman, J. B.; Cioslowski, J.; Stefanov, B. B.; Nanayakkara, A.; Challacombe, M.; Peng, C. Y.; Ayala, P. Y.; Chen, W.; Andres, J. L.; Replogle, E. S.; Gomperts, R.; Martin, R. L.; Fox, D. J.; Binkley, J. S.; Defress, D. J.; Baker, J.; Stewart, J. J. P.; Head-Gordon, M.; Gonzalez, C.; Pople, J. A. Gaussian 94; Gaussian, Inc.: Pittsburgh, PA, 1995.
- Pellerite, M. J.; Brauman, J. I. *J. Am. Chem. Soc.* **1980**, *102*, 5993.
- (a) Wolfe, S.; Mitchell, D. J.; Schlegel, H. B. *J. Am. Chem. Soc.* **1981**, *103*, 7692. (b) Shaik, S. S.; Schlegel, H. B.; Wolfe, S. *Theoretical Aspects of Physical Organic Chemistry. The S_N2 Mechanism*; Wiley: New York, 1972; Chapters 4-6.
- A transition structure corresponds to a saddle point on a theoretical potential energy surface (ΔE), whereas a transition state is a free energy (ΔG) maximum along the reaction coordinate and the two energies are related by eqs. 2.
- (a) Hammond, G. S. *J. Am. Chem. Soc.* **1955**, *77*, 334. (b) Leffler, J. E.; Grunwald, E. *Rates and Equilibria of Organic Reactions*; Wiley: New York, 1963. (c) Leffler, J. E. *Science* **1953**, *117*, 340.
- Dewar, M. J. S.; Dougherty, R. C. *The PMO Theory of Organic Chemistry*; Plenum: New York, 1975; p 212.

15. (a) Marcus, R. A. *Annu. Rev. Phys. Chem.* **1965**, 15, 155. (b) Cohen, A. O.; Marcus, R. A. *J. Phys. Chem.* **1968**, 72, 4249.
 16. (a) Kresge, A. J. *Acc. Chem. Res.* **1975**, 8, 354. (b) Jencks, W. P. *Chem. Rev.* **1985**, 85, 511. (c) Lowry, T. H.; Richardson, K. S. *Mechanism and Theory in Organic Chemistry*, 3rd ed.; Harper and Row: New York, 1987; p 671. (d) Ref. 11b, Chapter 1.
 17. (a) Pauling, L. *J. Am. Chem. Soc.*, **1947**, 69, 542. (b) Ford, G. P.; Smith, C. T. *J. Am. Chem. Soc.*, **1987**, 109, 1325. (c) Han, I.-S.; Kim C. K.; Kim, C. K.; Lee, B.-S.; Lee, I. *J. Comput. Chem.* **1997**, 18, 1773.
 18. (a) Bernasconi, C. F. *Acc. Chem. Res.* **1987**, 20, 301. (b) Bernasconi, C. F. *Acc. Chem. Res.* **1992**, 25, 9. (c) Bernasconi, C. F. *Adv. Phys. Org. Chem.* **1992**, 27, 116.
 19. Shi, Z.; Boyd, R. J. *J. Am. Chem. Soc.* **1991**, 113, 2434. The experimental value is 26.2 kcal mol⁻¹¹⁰ and the value at RHF/4-31G level is 11.7 kcal mol⁻¹.^{11a}
 20. The sp² hybridized carbon has a greater s-orbital character than the sp³ carbon so that forms a stronger bond (approx. bond energies of the sp² (ethylene) and sp³ carbon (methane) are 105.2 and 98.2 kcal mol⁻¹, and electronegativities are 2.75 and 2.48, respectively).²¹
 21. McWeery, R. *Coulson's Valence*; Oxford Univ. Press: Oxford, 1979; p 166 and 203.
 22. Ref. 11b, p 173.
-